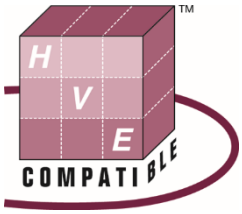

HVE-WP-2017-1

Development of a 12-Node Thermodynamic Simulation Model of a Disc Brake Assembly

Terry D. Day, P.E.
Engineering Dynamics Corporation

Reprinted From: 2017 HVE Forum White Paper Session

2017 HVE Forum
New Orleans, LA
March 6 – 10, 2017

8625 SW Cascade Avenue, Suite 200, Beaverton, OR 97008, USA Tel: 888.768.6216 www.edccorp.com

Persons wishing to submit papers to be considered for presentation or publication during an HVE Forum should send the manuscript or a 300 word abstract of a proposed manuscript to: Training Manager, Engineering Dynamics Corporation.

Development of a 12-Node Thermodynamic Simulation Model of a Disc Brake Assembly

Terry D. Day, P.E.
Engineering Dynamics Corporation

Abstract

Overheated brakes on a heavy truck can lead to a loss of braking and subsequent crash. This typically occurs after prolonged braking on a downhill grade. The problem is often accompanied by improper brake adjustment, causing one or more of the actuators to reach the end of travel due to thermal expansion. Reconstruction of this type of crash requires the consideration of overheated brakes. A thermodynamic model of a drum-type foundation brake is included in the HVE simulation environment and has been used successfully to study this phenomenon. However, newer on-highway trucks are often fitted with disc brakes. A similar thermodynamic model for a heavy truck disc brake does not exist, making the problem described above difficult to address. This paper describes a new thermodynamic model of a disc foundation brake, such as those often fitted on newer heavy trucks. The model is based on classic thermodynamic heat transfer principles that describe the rate of heat flow through the brake rotor and pads as a function of time and location within the rotor and pad materials. Simulation results are used to compare the new disc brake model with the existing drum brake model.

Introduction

Motor vehicle crashes in the US in 2014 killed 32675 people and injured about 2.34 million more [1,2]. Truck crashes are a relatively small percentage of the total crash population. Unfortunately, however, crashes involving heavy trucks are generally much more severe and have greater consequences in terms of both injury severity and cost.

The NTSB estimates that 1 to 2 percent of heavy truck crashes involve brakes that are out of adjustment [3]. Their research in the early 1990s revealed that when heavy trucks are randomly inspected on the highway, more that 50 percent of these vehicles have one or more brakes that fail to meet established adjustment criteria. This percentage is probably less today because of the use self-adjusting slack adjusters on air-braked heavy vehicles. However, the state and effect of brake adjustment is of primary concern in the reconstruction of heavy truck crashes.

Simulation tools are available to rigorously analyze the effect of adjustment on braking effectiveness (measured in either stopping distance or maximum achievable deceleration rate). One such tool, called the HVE Brake Designer [4], incorporates a thermodynamic model to calculate the temperature increase in a drum brake assembly. The temperature increase is accompanied by thermal expansion which increases the necessary stroke of the brake actuator (air chamber). If the initial state of adjustment is such that the available stroke is insufficient, brake torque is reduced and overall stopping distance (and deceleration) are increased. This phenomenon is commonly called brake fade.

The thermodynamic model in the Brake Designer assumes a drum-type brake assembly. However, modern heavy trucks are starting to use disc brakes. The thermodynamics of a disc brake differ from a drum brake. Therefore, the above analysis of brake fade does not apply to trucks fitted with disc brakes. A thermodynamic model of a disc brake is needed. This paper describes the development of a thermodynamic model of a disc brake assembly.

Prior Research

Thermodynamic modeling of drum and disc brakes is not new. The original temperature model for a drum brake, and the model after which the subject disc model was patterned, was described in [5]. That model provides the temperature at three locations: Lining/Drum interface, drum interior and lining interior. However, the model internally calculates the temperature at each of 13 nodes; 11 in the drum and 2 in the lining material.

Fancher [6] performed testing of two different on-highway heavy trucks, documenting lining and drum temperatures for a variety of braking conditions over long, down-hill grades. They also presented a set of heat flow equations for average cooling rate.

Limpert has published extensively on brake systems. In *Brake Design and Safety* [7], he includes an overview of brake thermodynamics, and also presents suggested values for heat transfer coefficients for various material used in wheel brake assemblies (see Table dd).

Emery [8] conducted braking tests on three vehicles that used front disc, rear drum brake systems to measure brake fluid and brake rotor/pad temperatures under varying operating conditions (vehicle speed, fluid moisture content, braking severity and length of brake application). The goal of this research was to help predict brake failure due to brake fluid moisture absorption.

FHWA supported several research projects that studied the effects of prolonged, down-hill braking on wheel brake temperatures [9, 10, 11]. Reference 11 is a user's manual for a computer program designed to predict wheel brake assembly temperatures of trucks on grade.

Roberts [12] presented the technical details for the Brake Designer, but did not go into the details of the thermodynamic portion of the model.

Ruhl [13, 14] presented an overview of several models, including those described above, and included a comparison of results from each model.

Finite element methods have also been used to model brake temperature. Three examples are [15, 16 and 17]. All three authors model the heat input into the brake as a function of change in kinetic energy (speed change) and/or potential energy (down-hill grade) of the total vehicle, apportioning the total heat energy for an individual wheel brake assembly according to vehicle weight distribution. These authors also presented suggested values for heat transfer coefficients.

Neys [18] presents a detailed description of the heat flow and resulting characteristic temperature variation in the individual components of a disc brake assembly. The primary goal of this research focuses ultimately on the temperature of the brake fluid and ways to ensure the fluid does not reach a vaporization temperature.

HVE Brake Designer

The HVE Brake Designer is a mechanical design/analysis tool that calculates brake torque ratio based on wheel brake component dimensions and material properties:

$$BTR = AF \times BF \times TR \quad (1)$$

where

BTR = brake torque ratio
AF = actuation factor
BF = brake factor
TR = torque radius

Brake torque ratio is a fundamental property that determines current brake torque at the wheel according to the mechanical properties of the wheel brake assembly (dimensions, materials and geometrical layout of the components) and the currently applied brake system pressure at the wheel. Mechanical analysis for both disc- and drum-type brakes is based on Limpert [7].

The actuation factor represents the actuation force per unit of brake system pressure, the actuation force being the force exerted by the wheel cylinder piston or air chamber to push the brake pads against the brake rotor (disc brake) or linings against the drum (drum brake).

A free-body analysis of a wheel brake assembly (either disc or drum) results in a dimensionless quantity called the brake factor. The brake factor is simply the ratio of the rubbing force between the rotor and pads (disc brake) or drum and linings (drum brake) and the brake actuator force (i.e., the force produced by the hydraulic piston or air chamber). For a disc brake, the brake factor is

$$BF = 2 \times \mu_P \quad (2)$$

where

μ_P= friction coefficient between the rotor and pads

For a drum brake, calculating the brake factor is significantly more complicated. The brake factor differs according to the type of drum brake assembly (duo-servo, two leading shoe, leading/trailing shoe, etc.). In general, the drum/lining friction coefficient, shoe geometry and actuator location all affect the brake factor. Reference 7 includes an equation for brake factor for each brake assembly type.

The torque radius is the distance from the wheel center to the rubbing surface. For a disc brake, the torque radius is

$$TR = \frac{R_o + R_i}{2} \quad (3)$$

where

R_o = disc outer radius
R_i = disc inner radius

The torque radius for a drum brake is simply the rubbing radius (half of the drum diameter).

Material and thermodynamic properties for the rotor and pads (disc brake) and drum and linings (drum brake) are also required. Friction vs. pad/lining temperature is also provided.

See references 4 and 11 for a complete description of the Brake Designer.

Drum Brake Temperature Model

The existing temperature model uses 13 nodes (see Figure 1) that describe the temperature profile across a drum brake assembly. The model includes 11 nodes for the drum and 2 nodes for the lining. Heat energy enters the system at the lining/drum interface. The current energy into the system is

$$\dot{Q} = T_w \times \omega \quad (4)$$

where

$\dot{Q}$ = rate of heat energy (work) into brake assembly
T_w= current brake torque
ω= current wheel spin velocity

The heat energy is dissipated through conduction, convection and thermal capacitance of the lining and drum. The output of the model is the current temperature at each node. The current values for lining/drum interface temperature, lining internal temperature and drum internal temperature are displayed as outputs.

Disc Brake Temperature Model

The temperature model for a disc brake uses the same basic concepts as the existing drum brake model, that is, a multi-node model that calculates the current temperature across the disc brake cross-section. The disc brake model is a 12-node model shown in Figure 2. Like the drum brake model, the disc brake modeling procedure allows for the analysis of both internal and surface temperatures of the rotor and pads, as well as the temperature at the inner and outer rotor/pad interfaces where brake torque is produced. Rotor and pad internal temperatures and rotor/pad interface temperatures are displayed as outputs.

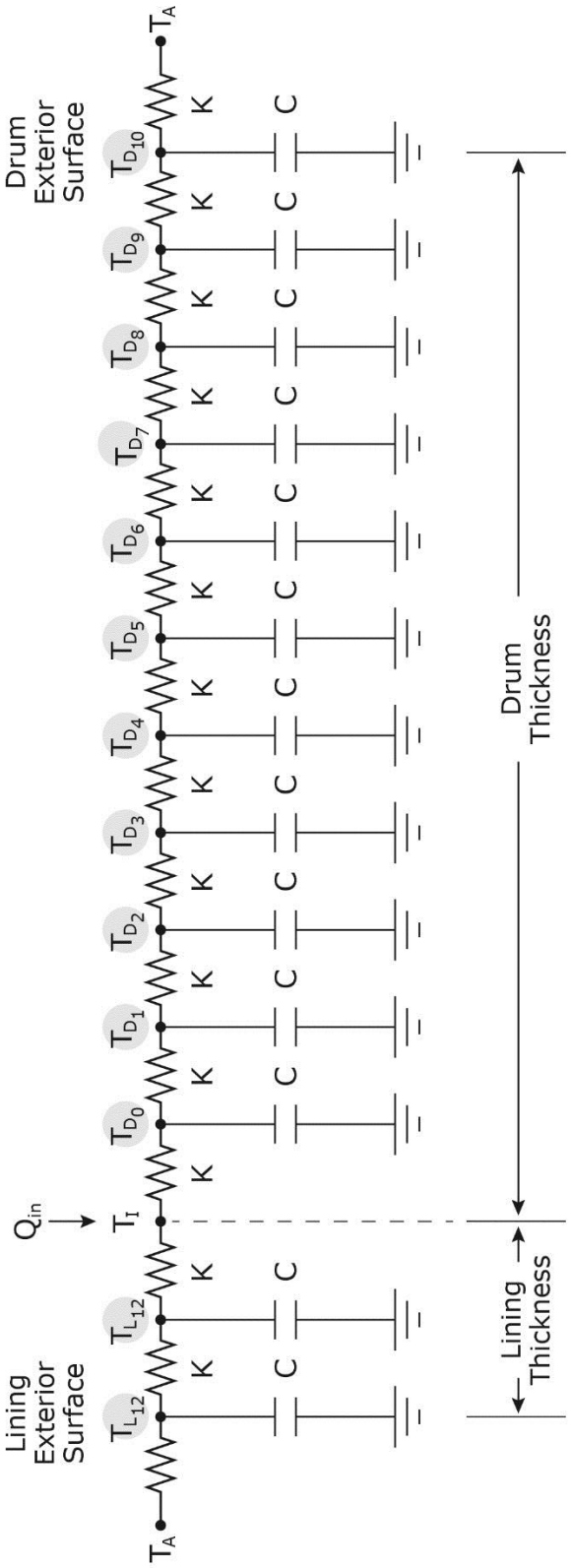

Figure 1 – 13 node lumped mass drum brake thermodynamic model used by the HVE Brake Designer

Heat Transfer Equations

The method and its solution are derived from the First Law of Thermodynamics: the total energy within a closed system remains constant (this is the thermodynamic version of the Conservation of Energy). Using this approach, an energy balance is applied to each of the 12 nodes shown in Figure 2. An overview of this procedure follows. In this development, the term "lump" identifies a volume of brake material (either rotor or pad). A "node" is the point within the lump volume where the temperature is calculated by the model. For programmatic reasons, node indices are 0-based. Thus, node 0 will be inside of lump 1, and so forth.

Rotor

The disc rotor is divided into eight lumps of equal thickness. The thickness of each lump is simply the rotor thickness divided by the number of lumps.

The first and eighth lumps have surfaces that are exposed to the ambient air. The surfaces of these lumps are also in contact with the disc brake pads on either side of the rotor.

An energy balance for node 0 is shown in Figure 3. This figure illustrates the general concept that the energy into the lump is equal to the energy out of the lump plus the energy stored inside the lump.

The individual heat flows may be expressed in terms of their boundary temperatures, T, and their heat transfer coefficients, K (conduction), H (convection) and C (capacitance).

Analysis of the energy balance for the temperature, T_{R_0}, at node 0 is

$$\frac{dQ}{dt_{S_1}} + \frac{dQ}{dt_1} = \frac{dQ}{dt_1} + \frac{dQ}{dt_{R_0}} \tag{5}$$

where

$$\frac{dQ}{dt_{S_1}} = K_{S_1}\left(T_{R_{S_1}} - T_{R_0}\right) \tag{6}$$

$$\frac{dQ}{dt_I} = K_I\left(T_I - T_{R_0}\right) \tag{7}$$

$$\frac{dQ}{dt_1} = K\left(T_{R_0} - T'_1\right) \tag{8}$$

$$\frac{dQ}{dt_{R_0}} = C\frac{dT}{dt_{R_0}} \tag{9}$$

Substituting (6) through (9) into (5) yields

$$K\left(T_{R_{S_1}} - T_{R_0}\right) + K_I\left(T_I - T_{R_0}\right) = K\left(T_{R_0} - T'_1\right) + C\frac{dT}{dt_{R_0}} \tag{10}$$

The temperature, T'_1, at the boundary between lumps 1 and 2 is the average temperature (assuming K is the same for both lumps), so

$$T'_1 = \frac{T_{R_0} + T_{R_1}}{2} \tag{11}$$

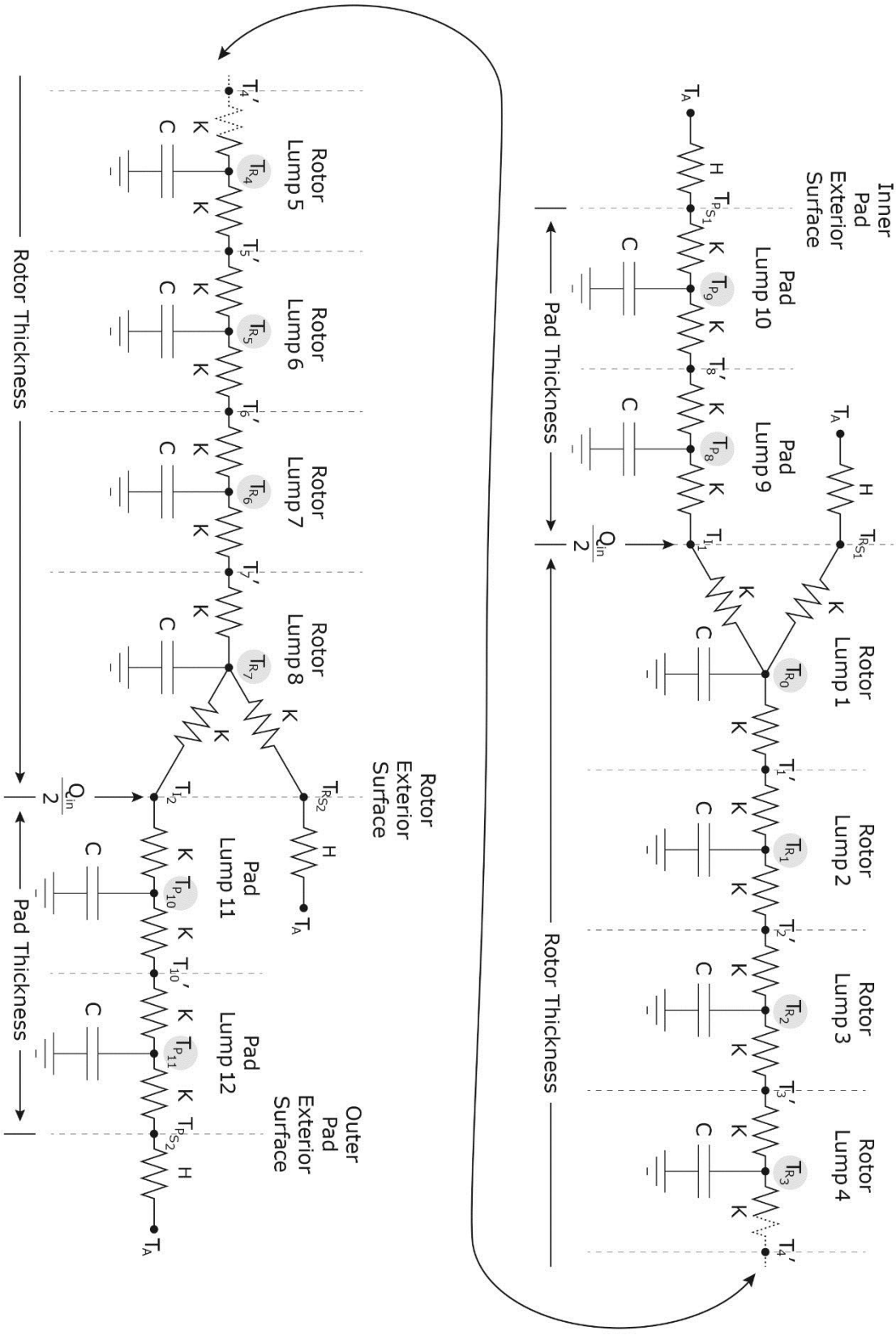

Figure 2 – 12-node lumped mass thermodynamic model for a disc brake used by the HVE Brake Designer

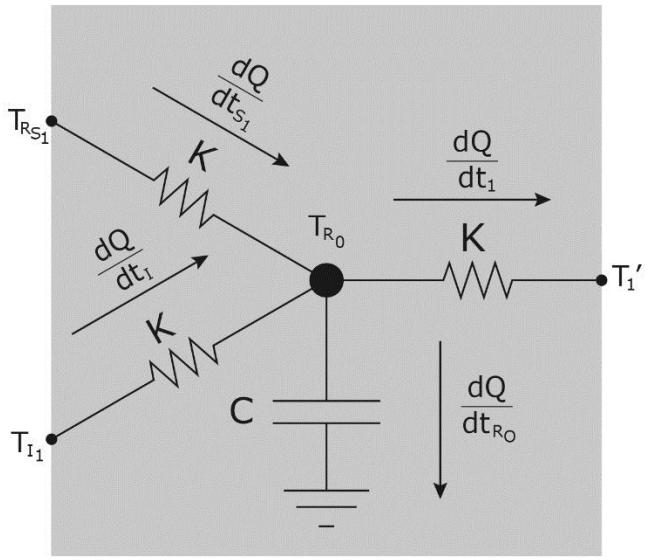

Figure 3 – Energy balance for lump 1 (see also Figure 2)

The temperature at the rotor surface, $T_{R_{S_1}}$, is not an independent value; it is dependent upon the temperature of Node 0, T_{R_0}, ambient temperature, T_A, and conduction and convection coefficients, K and H, respectively. An energy balance for inner rotor exterior surface is shown in Figure 4.

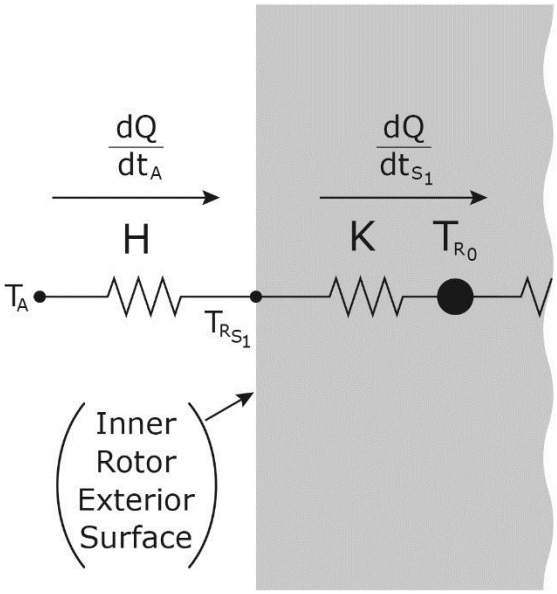

Figure 4 – Energy balance for the inner rotor exterior surface (see also Figure 2)

Analysis of the temperature at the rotor surface is

$$\frac{dQ}{dt_A} = \frac{dQ}{dt_{S_1}} \tag{12}$$

where

$$\frac{dQ}{dt_A} = H\left(T_A - T_{R_{S_1}}\right) \tag{13}$$

$$\frac{dQ}{dt_{S_1}} = K_{S_1}\left(T_{R_{S_1}} - T_{R_0}\right) \tag{14}$$

Substituting (13) and (14) into (12) yields

$$H\left(T_A - T_{R_{S_1}}\right) = K_{S_1}\left(T_{R_{S_1}} - T_{R_0}\right) \tag{15}$$

Solving for $T_{R_{S_1}}$,

$$T_{R_{S_1}} = \left(\frac{HT_A + K_{S_1}T_{R_0}}{H + K_{S_1}}\right) \tag{16}$$

Rearranging (10), substituting (11) and (16), and solving for $\frac{dT}{dt_{R_0}}$ yields

$$\frac{dT}{dt_{R_0}} = \frac{K}{C}\left(\frac{K}{H+K} - \frac{5}{2}\right)T_{R_0} + \frac{K}{2C}T_{R_1} + \frac{K}{C}\left(\frac{H}{H+K}\right)T_A + \frac{K}{C}T_I \tag{17}$$

Lumps 2 through 6 are internal, sandwiched between lumps 1 and 7. An energy balance for lump 2 (the development for nodes 3 through 7 is identical) is shown in Figure 5.

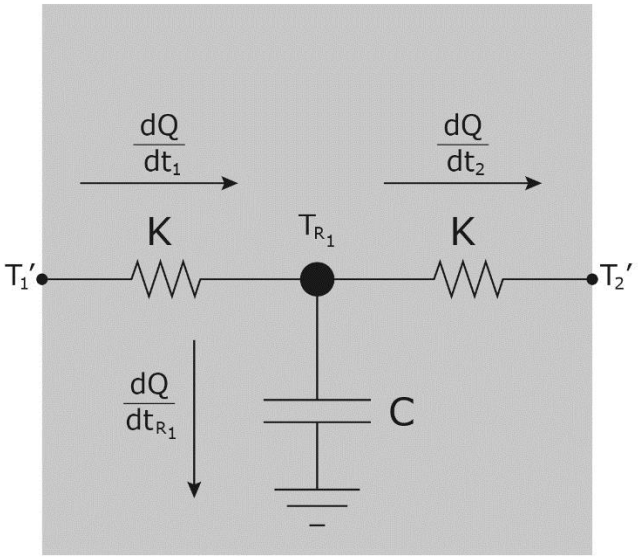

Figure 5 – Energy balance for lump 2 (lumps 3 through 7 are similar)

Analysis of this energy balance for the temperature, T_{R_1}, at node 1 is

$$\frac{dQ}{dt_1} = \frac{dQ}{dt_2} + \frac{dQ}{dt_{R_1}} \tag{18}$$

where

$$\frac{dQ}{dt_1} = K\left(T_1{}' - T_{R_1}\right) \quad (19)$$

$$\frac{dQ}{dt_2} = K\left(T_{R_1} - T_2{}'\right) \quad (20)$$

$$\frac{dQ}{dt_{R_1}} = C\frac{dT}{dt_{R_1}} \quad (21)$$

Substituting (19) through (21) into (18) yields

$$K\left(T_1{}' - T_{R_1}\right) = K\left(T_{R_1} - T_2{}'\right) + C\left(\frac{dT}{dt_{R_1}}\right) \quad (22)$$

Solving for $\frac{dT}{dt_{R_1}}$,

$$\frac{dT}{dt_{R_1}} = \frac{K}{C}\left(T_1{}' - 2T_{R_1} + T_2{}'\right) \quad (23)$$

Again noting that the temperature at the boundary between two lumps of the same material is the average temperature of the two lumps (see eq. 11), substitution yields

$$\frac{dT}{dt_{R_1}} = \frac{K}{C}\left(\frac{T_{R_0}}{2} - T_{R_1} + \frac{T_{R_2}}{2}\right) \quad (24)$$

Analysis of the temperatures at nodes 2 through 6 follows the same procedure shown in eqns. (18) through (24), resulting in a general expression for each node, n, in this range,

$$\frac{dT}{dt_{R_n}} = \frac{K}{C}\left(\frac{T_{R_{n-1}}}{2} - T_{R_n} + \frac{T_{R_{n+1}}}{2}\right) \quad (25)$$

Pads

A disc brake has an inner and outer pad. Each pad is divided into two lumps of equal thickness (pad thickness divided by 2).

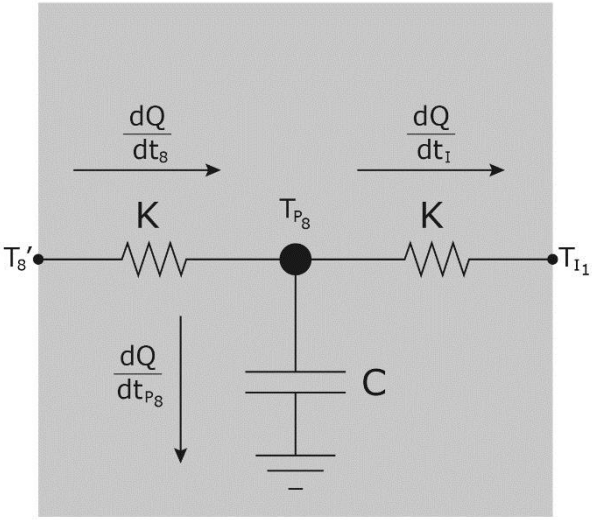

Figure 6 – Energy balance for lump 9 at the inner pad/rotor interface

Lumps 9 and 10 are for the inside pad; Lumps 11 and 12 are for the outside pad. Lumps 9 and 11 are in contact with the disc rotor; lumps 10 and 12 are exposed to ambient air.

An energy balance for lump 9 is shown in Figure 6. Analysis of this energy balance for the temperature, T_{P_8}, at node 8 is

$$\frac{dQ}{dt_8} = \frac{dQ}{dt_{P_8}} + \frac{dQ}{dt_{I_1}} \quad (26)$$

where

$$\frac{dQ}{dt_8} = K\left(T_8{}' - T_{P_8}\right) \quad (27)$$

$$\frac{dQ}{dt_{P_8}} = K\left(T_{P_8} - T_{I_1}\right) \quad (28)$$

$$\frac{dQ}{dt_{I_1}} = C\frac{dT}{dt_{P_8}} \quad (29)$$

Substituting (27) through (29) into (26) yields

$$K\left(T_8{}' - T_{P_8}\right) = K\left(T_{P_8} - T_{I_1}\right) + C\frac{dT}{dt_{P_8}} \quad (30)$$

$T_8{}'$ is the average of the neighboring node temperatures, so

$$T_8{}' = \frac{T_{P_8} + T_{P_9}}{2} \quad (31)$$

Substituting (31) into (30) and rearranging yields

$$\frac{dT}{dt_{P_8}} = \frac{K}{C}\left(-\frac{3}{2}T_{P_8} + \frac{1}{2}T_{P_9} + T_{I_1}\right) \quad (32)$$

The temperature, $T_{P_{10}}$, at node 10 (outer pad) follows the same procedure, resulting in

$$\frac{dT}{dt_{P_{10}}} = \frac{K}{C}\left(-\frac{3}{2}T_{P_{10}} + \frac{1}{2}T_{P_{11}} + T_{I_2}\right) \quad (33)$$

Pad lumps 10 and 12 are exposed to ambient air. An energy balance for lump 10 is shown in Figure 7. Analysis of this energy balance for the temperature, T_{P_9}, at node 9 is

$$\frac{dQ}{dt_9} = \frac{dQ}{dt_8} + \frac{dQ}{dt_{P_9}} \quad (34)$$

where

$$\frac{dQ}{dt_9} = K\left(T_{P_{S_1}} - T_{P_9}\right) \quad (35)$$

$$\frac{dQ}{dt_8} = K\left(T_{P_9} - T_8{}'\right) \quad (36)$$

$$\frac{dQ}{dt_{P_9}} = C\frac{dT}{dt_{P_9}} \quad (37)$$

Substituting (35) through (37) into (34) yields

$$K\left(T_{P_{S_1}} - T_{P_9}\right) = K\left(T_{P_9} - T_8{}'\right) + C\frac{dT}{dt_{P_9}} \quad (38)$$

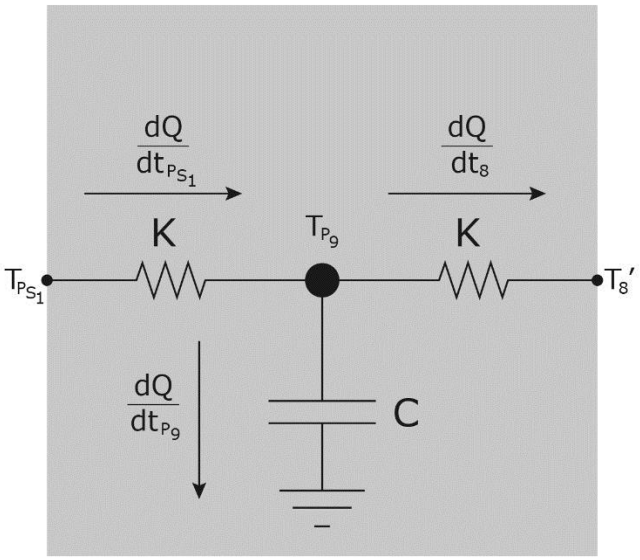

Figure 7 – Energy balance for the lump 10 (see also Figure 2)

Solving for $\frac{dT}{dt_{P_9}}$.

$$\frac{dT}{dt_{P_9}} = \frac{K}{C}\left(T_{P_{S_1}} - 2T_{P_9} + T_8{}'\right) \tag{39}$$

As previously shown,

$$T_8{}' = \frac{T_{P_8}+T_{P_9}}{2} \tag{40}$$

and

$$T_{P_{S_1}} = \frac{HT_A+KT_{P_9}}{H+K} \tag{41}$$

Substituting (40) and (41) into (39) yields

$$\frac{dT}{dt_{P_9}} = \frac{K}{C}\left(\frac{H}{H+K}T_A + \left(\frac{K}{H+K} - \frac{3}{2}\right)T_{P_9} + \frac{1}{2}T_{P_8}\right) \tag{42}$$

The temperature, $T_{P_{11}}$, at node 11 (outer pad) follows the same procedure, resulting in

$$\frac{dT}{dt_{P_{11}}} = \frac{K}{C}\left(\frac{H}{H+K}T_A + \left(\frac{K}{H+K} - \frac{3}{2}\right)T_{P_{11}} + \frac{1}{2}T_{P_{10}}\right) \tag{43}$$

Pad-Rotor Interface

The frictional interface between the rotor and the pads is important because the braking energy enters the brake assembly at that location. An energy balance for the interface between the inner pad and the rotor is shown in Figure 8.

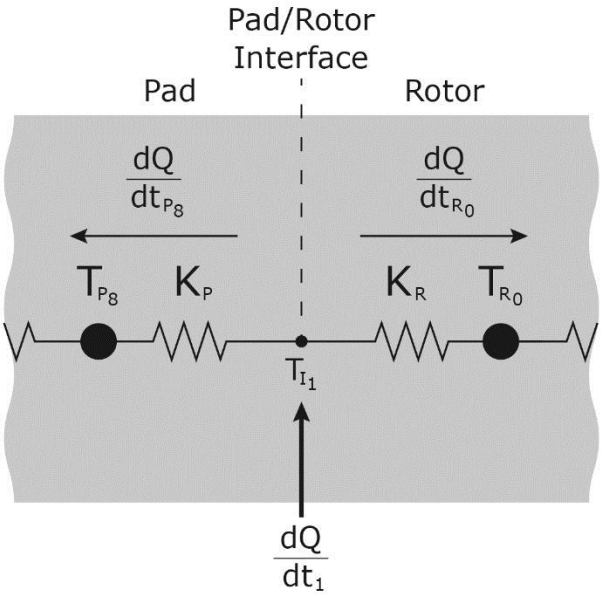

Figure 8 – Energy balance at the inner pad-rotor interface (see also Figure 2). One half of the brake thermal energy enters here. The other half enters at the outer pad/rotor interface.

Analysis of this energy balance provides the solution for the temperature at the interface, T_{I_1}

$$\frac{dQ}{dt_1} = \frac{dQ}{dt_{P_8}} + \frac{dQ}{dt_{R_0}} \tag{44}$$

where

$$\frac{dQ}{dt_1} = \dot{Q}_{\text{in1}} \tag{45}$$

$$\frac{dQ}{dt_{P_8}} = K_P\left(T_{I_1} - T_{P_8}\right) \tag{46}$$

$$\frac{dQ}{dt_{R_0}} = K_R\left(T_{I_1} - T_{R_0}\right) \tag{47}$$

Substituting and solving for T_{I_1} yields

$$T_{I_1} = \frac{\dot{Q_{in1}}+K_PT_{P_8}+K_RT_{R_0}}{K_P+K_R} \tag{48}$$

A similar analysis of the outer pad-rotor interface results in

$$T_{I_2} = \frac{\dot{Q_{in2}}+K_PT_{P_{10}}+K_RT_{R_7}}{K_P+K_R}$$

Solution Procedure

The differential equation describing the heat flow through the brake assembly is of the form

$$M\dot{T} = ST + CT_I + DT_A \tag{49}$$

where

M	= Thermal mass
$\dot{T}$	= Rate of temperature change
S	= Thermal conduction and convection
T	= Node temperature
C	= Thermal conduction at rotor/pad interface
T_I	= Rotor/pad interface temperature
D	= Rotor and pad thermal convection
T_A	= Ambient temperature

Equation 49 is solved for $\dot{T}$ at each of the 12 nodes. The formulation is conveniently expressed in matrix form, where

$$[\bar{S}] = [S][M]^T$$
$$[\bar{C}] = [C][M]^T$$
$$[\bar{D}] = [D][M]^T$$

Conduction, Convection and Capacitance Coefficients

The individual coefficients for the heat transfer equations are described below.

Rotor

The rotor is divided into eight lumps of equal thickness. The conduction coefficients for rotor node, n, are

$$K_{n_{Rotor}} = \frac{K_{T_{Rotor}} A_{Rotor}}{x} = \frac{K_{T_{Rotor}} A_{Rotor}}{th_{Rotor}/2N_{Nodes_{Rotor}}} = \frac{16 K_{T_{Rotor}} A_{Rotor}}{th_{Rotor}}$$

The convection coefficients for rotor node, n, are

$$H_{n_{Rotor}} = \left(H_{0_{Rotor}} + H_{V_{Rotor}} V_{Wheel}\right) A_{Rotor}$$

The capacitance coefficients for rotor node, n, are

$$C_{n_{Rotor}} = \frac{C_{p_{Rotor}} Mass_{Rotor}}{N_{Nodes_{Rotor}}} = \frac{C_{p_{Rotor}} Mass_{Rotor}}{8}$$

where

$N_{Nodes_{Rotor}}$	= 8
A_{Rotor}	= Cross-sectional area of rotor

Pads

The inner and outer pads are each divided into two lumps of equal thickness. The conduction coefficients for pad node, n, are

$$K_{n_{Pad}} = \frac{K_{T_{Pad}} A_{Pad}}{x} = \frac{K_{T_{Pad}} A_{Pad}}{th_{Pad}/2N_{Nodes_{Pad}}} = \frac{4 K_{T_{Pad}} A_{Pad}}{th_{Pad}}$$

The convection coefficients for pad node, n, are

$$H_{n_{Pad}} = \left(H_{0_{Pad}} + H_{V_{Pad}} V_{Wheel}\right) A_{Pad}$$

The capacitance coefficients for rotor node, n, are

$$C_{n_{Pad}} = \frac{C_{p_{Pad}} Mass_{Pad}}{N_{Nodes_{Pad}}} = \frac{C_{p_{Pad}} Mass_{Pad}}{2}$$

where

$N_{Nodes_{Pad}}$	= 2
A_{Pad}	= Cross-sectional area of pad

Parameter Estimation

Brake rotors, like drums, are almost always made of cast iron alloys. Conduction coefficients, K, specific heat, C_p (for capacitance), and density, ρ, for cast iron are well known and may be found in numerous engineering handbooks, as well as reference 7.

Brake pads, once made from asbestos, are now made from phenolic resins with steel or aramid fibers (for strength and wear resistance) and fillers and binders. Coefficients and density for these materials are mostly proprietary. The default values for K, C_p, and density, ρ, are based on published values for asbestos. It should be noted that values for phenolic pads and linings are expected to be slightly higher [7].

Convection characteristics are less well established. Convection is dependent upon air flow across a surface (in this case, the rotor and pad exterior surfaces). This air flow is dependent upon installation geometry (exposure to air flow) and the speed of the air across the surfaces (obviously related to vehicle speed).

Convection in the HVE Brake Designer includes a static coefficient, H_0 and a velocity-dependent coefficient, H_v Values for H_0 come from [7]. The default value for H_v is set to 0. The model is intended to encourage research to establish a reasonable velocity-dependent contribution to convective brake cooling.

Table 1 summarizes the thermodynamic heat transfer properties for standard materials used in brake assemblies.

Dimensions (material volume and thickness and exposed surface areas) are derived directly from the design dialogs in the HVE Brake Designer.

Vented Rotors

The 8-node rotor model does not currently accommodate a vented rotor. A vented rotor may be approximated by increasing the standard convection coefficient by approximately 50% [7].

Simulation

The operational characteristics of the wheel brake assembly created using the Brake Designer can be tested directly using simulation. A simulation event can be set up to recreate a desired scenario, e.g., a heavy truck on a long, down-hill grade. The state of brake adjustment (slack adjuster stroke) at each wheel can be varied to determine if/how the state of adjustment was a factor in a loss of braking. The

Table 1 – Material thermodynamic properties for disc brake pads and rotors [7, 21]. See also [15, 16, 17]

Material Properties		
	Pad	Rotor
Density, ρ $(\frac{lb}{ft^3})$	162.3	454.5 (cast iron)
Specific Heat, C_p $(\frac{BTU}{lb-\ ^oF})$	0.35	0.10
Conduction, K $(\frac{BTU}{ft-hr-\ ^oF})$	0.67	26.8 (cast iron)
Convection, H $(\frac{BTU}{ft^2-hr-\ ^oF})$	7 - 20	7 – 20 (solid) 14 – 40 (vented)

brake torque produced by an out-of-adjustment drum brake is reduced as the temperature increases and the drum expands. This phenomenon is well-modeled by the Brake Designer.

Future Work

A validation effort is underway. HVE brake temperature simulation results are compared directly with results from brake dynamometer tests.

Additional validations compare HVE brake temperature simulations with other research [6, 13].

These results will be published in a future technical report.

Discussion

Disc vs. Drum Differences

The operational differences between disc and drum brakes are quite interesting. In a drum brake, heating causes the drum to expand away from the linings, thus requiring an increase in actuator stroke. If the state of adjustment for a wheel's brake is such that the actuator (air chamber push rod) approaches the end of its travel (typically 2.5 to 3.5 inches), the actuator force is reduced, resulting in reduced brake torque. This is commonly called brake fade, and can be a significant problem for heavy trucks on a long downhill grade. Thermal expansion in a disc brake actually increases clamping force between the rotor and pads. Thus, a disc brake is virtually immune to brake fade unless the pad temperature increases to the point where the fillers and binders in the pad break down; this can be expected to occur at temperatures above 600 degrees Fahrenheit [7].

Drum brake torque increases in a non-linear manner as friction increases. Disc brake torque is perfectly linear with increased friction. The linear relationship results in a more consistent braking between right- and left-side wheels and between front and rear axles. A vehicle fitted with disc brakes is more likely to stop straighter and is less prone to unexpected wheel lock-up. These important brake system attributes lead to greater stability during heavy braking of a vehicle fitted with disc brakes.

The thermodynamic analysis presented earlier in this paper provides some interesting observations. The rubbing surfaces of a disc brake are fully exposed to surrounding air, whereas the rubbing surface of a drum brake is typically enclosed. Also, a disc brake has two rubbing surface (each absorbing about half of the total heat load from braking), whereas a drum brake has only one rubbing surface. Therefore, disc brakes are inherently better cooled than drum brakes. It is also worth noting that the rubbing surface is the hottest part of the brake. Being directly exposed to cooling air helps to further reduce both rotor and pad temperatures.

There are two disadvantages of disc brakes. First, because they have a smaller brake factor, disc brakes require higher brake system pressures. Second, they tend to be more expensive to manufacture, often requiring a secondary system to serve as a parking brake.

Air vs. Hydraulic Actuator Differences

A conventional hydraulic disc brake used on passenger vehicles and light trucks uses hydraulic (fluid) pressure to create the clamping force between the pads and rotor. Hydraulic pressure pushes one or two pistons against the back of the pad on one side which creates the clamping force against the rotor to create brake torque. It is possible that heat transfer through the pad can make its way to the piston and then to the hydraulic fluid, raising its temperature. This can cause the fluid to vaporize and lead to a loss of braking [8].

Air disc brakes used on heavy trucks use a different actuator design: The pressure in the air chamber (type 24 chambers are typically used) applies a pushrod force against the end of a lever. This lever has a large mechanical advantage; typically about 15:1 [19]. The other end of the lever pushes against back of the pad (effectively replacing the piston in a hydraulic disc brake assembly). This design eliminates the potential for loss of actuator force due to high temperature. See [19, 20] for a good overview of air disc brake design.

Summary

This white paper presents the initial publication describing a new thermodynamic model for a disc brake assembly. The heat transfer equations and their solution are presented in detail. Parameter estimation is provided. A discussion of the operational differences between disc- and drum-type brakes is also provided. Validation and related simulations are in progress and will be presented in a future technical report.

References

1. Traffic Safety Facts, 2014 Motor Vehicle Crashes: Overview, National Highway Traffic Safety Administration, DOT HS 812 246, Washington, DC, March 2016.
2. Traffic Safety Facts, 2014 Large Trucks, National Highway Traffic Safety Administration, DOT HS 812 246, Washington, DC, March 2016.
3. Heavy Vehicle Airbrake Performance, National Transportation Safety Board, NTSB/SS-92-01.
4. HVE User's Manual Engineering Dynamics Corporation, Beaverton, OR 2005.
5. MacAdam, C.C., Fancher, P.S., Hu, Garrick T., and Gillespie, T.D., A Computerized Model for Simulating the Braking and Steering Dynamics of Trucks, Tractor-semi-trailers, Doubles, and Triples Combinations, Highway Safety Research Institute, University of Michigan, Ann Arbor, Report No. UM-HSRI-80-58, 1980.
6. Fancher, P., Winkler, C., and Campbell, M., Influence of Braking Strategy on Brake Temperature in Mountain Descents, Transportation Research Institute, University of Michigan, Ann Arbor, 1992.
7. Limpert, R., Brake Design and Safety, Second Edition, Society of Automotive Engineers, Warrendale, PA, 1999.
8. Emery, A., Kumar, P., and Firey, J., Experimental Study of Automotive Brake System Temperatures, Washington State Department of Transportation, WA-RD 434.1,
9. Johnson, W., DiMarco, R., and Allen, W., The Development and Evaluation of a Prototype Grade Severity Rating System, FHWA-RD-81-185, Federal Highway Administration, Washington DC, 1982.
10. Hanscom, F., Field Test of the Grade Severity Rating System, FHWA-RD-86-011, , Federal Highway Administration, Washington DC, 1985.
11. Bowman, B., Grade Severity Rating System (GCSS) – User's Manual, FHWA-IP-88-015, Federal Highway Administration, Washington DC, 1989.
12. Roberts, S., and Day, T., Integrating Design and Virtual Test Environments for Brake Component Design and Material Selection," SAE 2000-01-1294, Society of Automotive Engineers, Inc., Warrendale, PA, 2000.
13. Ruhl, R., Inendino, L., and Southcombe, E., Comparison of Established Heavy Brake Heating/Cooling Models with HVE Brake Designer in a Real Mountain Accident, SAE Paper No. 2006-01-3556, Society of Automotive Engineers, Inc., Warrendale, PA 2006.
14. Ruhl, R. L., Inendino, L., Southcombe, E., and Ruhl, R.A., Useable Models for Free and Forced Cooling of Commercial Vehicle Drum Brakes, SAE Paper No. 2006-01-3557, Society of Automotive Engineers, Inc., Warrendale, PA 2006.
15. Belhocine, A., Cho, C., Nouby, M., Yi, Y., and Baker, A., Thermal Analysis of both Ventilated and Full Disc Brake Rotors with Frictional Heat Generation, Applied and Computational Mechanics, 8 (2014) 5-24, University of West Bohemia, 2014.
16. Talati, F., Jalalifar, S., Analysis of Heat Conduction in a Disk Brake System, Heat Mass Transfer, DOI 10.1007/s00231-009-0476-y, Springer-Verlag, 2009.
17. Manjunath, T., and Suresh, P., Structural and Thermal Analysis of Rotor Disc of Disc Brake, Department of Mechanical Engineering, KSIT, Bangalore, Karnataka, India, International Journal of Innovative Research in Science, Engineering and Technology, Volume 2, Issue 12. 2013.
18. Neys, A., In-Vehicle Brake System Temperature Model, Report No. 2012:38, Department of Applied Mechanics, Chalmers University of Technology, Göteborg, Sweden, 2012.
19. Ronald B. Heusser, Air Disc Brakes – Analysis, PowerPoint presentation at WREX 2016, Orlando, FL, May 2016.
20. http://www.FoundationBrakes.com.
21. Standard Handbook for Mechanical Engineers, Baumeister and Marks, Seventh Edition, McGraw-Hill, New York, 1967.

Acknowledgement

The author wishes to express his sincere appreciation to Paul Fancher, at The University of Michigan Transportation Research Institute, for his communication regarding the development of the original Phase 4 drum brake temperature model. That communication served as the basis for the development of the disc brake model described in this paper